Optical activity in the incommensurate structure Rb_2ZnBr_4

H. Meekes
Research Institute for Materials, University of Nijmegen, Toernooiveld, NL-6525 ED Nijmegen, The Netherlands

A. Janner
Institute of Theoretical Physics, University of Nijmegen, Toernooiveld, NL-6525 ED Nijmegen, The Netherlands
(Received 25 April 1988)

The optical activity in Rb_2ZnBr_4 crystals has been measured along three directions in a temperature interval from above 400 K down to 50 K. In the incommensurate phase already a nonvanishing element of the gyration tensor has been observed, despite the fact that the average crystal structure has inversion symmetry. In order to explain this, phenomenological space-dependent dielectric and gyration tensors, being invariant with respect to the superspace group of Rb_2ZnBr_4, have been considered. The selection rules imposed by symmetry, when compared with the experimental results, give a first indication on which long-wavelength Fourier components of these tensors are eventually responsible for the optical activity observed. A generalization of our considerations to other incommensurate structures is discussed.

I. INTRODUCTION

Rb_2ZnBr_4 is a member of the large family of A_2BX_4 dielectrics, which show a variety of phase transitions between different modulated phases. Many of these dielectrics—including Rb_2ZnBr_4—have an incommensurately modulated phase in a certain temperature range.[1] For an understanding of the mechanisms responsible for the phase transitions in these materials, a knowledge of the symmetry properties of the different phases is of great importance. Especially in the incommensurate phase, where a normal space-group description is not possible, a study of the symmetry properties is interesting as one can test the validity of the so-called superspace-group description.[2] These superspace groups have already been very useful for an understanding of a number of physical properties both in incommensurate and commensurate phases.[3]

The determination of optical activity—a third-rank-tensorial property of crystals—is a powerful tool for finding certain symmetry properties of crystals. By this means one tests, on the scale of the wavelength of the light used, for example, the presence of an inversion center or a mirror plane. Although the precise measurement of optical activity for directions other than the optical axes of the crystal has been very difficult, the introduction by Kobayashi and Uesu of a new type of polarimeter [high-accuracy universal polarimeter (HAUP)] made the measurement much more reliable and versatile.[4] We have measured the optical activity of Rb_2ZnBr_4 in three independent directions, in order to be able to compare the superspace description with another more conventional approach, which makes use of the symmetry of an average structure in the incommensurate phase, perturbed by the modulation.

Our specific choice for Rb_2ZnBr_4 was made for several reasons. First of all, the symmetry of the incommensurate phase has not been determined very conclusively in spite of great effort and the presence of structural characteristics shared with many other compounds of the same A_2BX_4 family.[5] Secondly, this crystal has several low-temperature phases, of which the structure is even more unclear,[6–8] and, thirdly, no measurement of optical activity of this compound has been reported up to now, whereas that is not the case for other members of the family.

One has, however, to note that there is a $(3+1)$-dimensional superspace group fitting the best with the experimental results, not only for Rb_2ZnBr_4.', but also for most of the other A_2BX_4 compounds. This superspace group, moreover, contains as maximum Euclidean subgroups the space groups of very many of the commensurate modulated phases observed. This is not accidental: simple interaction models allow one to understand the common structural features.[1] For all these reasons we have adopted the superspace group [denoted $Pcmn(00\gamma)(ss\bar{1})$] as being the symmetry group of the incommensurate phase of Rb_2ZnBr_4. The aim of the paper is to analyze whether such a symmetry group is compatible with the experimental data on optical activity. The challenge of such an aim is represented by the simple fact that both the space group of the average structure (*Pcmn*) and the above superspace group are centrosymmetric. To adopt the point of view that the symmetry group is a lower one missing a center of inversion is very tempting, but not consistent (in a simple way) with very many other experimental results.

This paper is organized as follows. In Sec. II we will give a description of the sequence of phases in Rb_2ZnBr_4 and an overview of alternative approaches for the optical activity, with special attention to the incommensurate phase. In Sec. III we will treat the symmetry properties of both the dielectric and the gyration tensor in the superspace approach. The next section deals with the experimental details including the evaluation procedure used for the results. A discussion of these results is given in Sec. V and, finally, we will give a conclusion.

II. OPTICAL ACTIVITY IN Rb_2ZnBr_4

The setting we will use will be the one chosen by Hogervorst in his comparative study of the modulated structures of the A_2BX_4 family,[1] for which, at room temperature, $a=13.33$ Å, $b=7.66$ Å, and $c=9.71$ Å, with basic space group $Pcmn$. Rb_2ZnBr_4 has a paraelectric phase between the melting point (753 K) and the incommensurate phase transition (347 K). The incommensurate modulation consists mainly of rotations of the $ZnBr_4^{2-}$ tetrahedra, combined with small shifts of all ions along the **b** axis,[5] the modulation wave vector being along $\mathbf{c}^*$: $\mathbf{q}=\gamma\mathbf{c}^*$ ($\gamma\approx 0.293$).[9] At $T_c=190$ K the wave vector jumps from its rather constant value in the incommensurate phase to the value $\gamma=\frac{1}{3}$, resulting in a commensurate ferroelectric[6] threefold superstructure (lock-in phase) between T_c and $T_3=112$K (F phase). At T_3 a new phase transition (to phase IV) appears, as van Kleef *et al.*[6] concluded from measurements of the dielectric constant. The symmetry in phase IV, however, does not differ from the lock-in (phase-III) symmetry. The structure of the lowest-temperature phases (phase V between 77 and 50 K and phase VI below 50 K) is not very clear. According to Ueda *et al.*,[8] the rational value of γ stays $\frac{1}{3}$, only some symmetry elements being lost.

See Table I for an overview of the expected symmetry groups and some measured properties.

With the use of the point-group symmetry of the structure in the different commensurate phases, one can easily predict which elements of the gyration tensor (g_{ij}) are expected to be zero (see, for example, Nye[10] and further on in this section). The results are summarized in Table II. Here we find that for temperatures below 77 K both g_{12} and g_{13} need not to be equal to zero, if we assume an m_x point symmetry, while between 77 and 347 K this holds only for g_{13}. In the high-temperature paraelectric phase the gyration tensor is zero because the point group is centrosymmetric.

In the incommensurate phase the normal space-group description is not adequate for the analysis of the gyration tensor. Instead of the normal three-dimensional space group, one can, however, make use of higher-dimensional space groups, with the aid of which the lattice-translational symmetry of the crystal can be restored.[2] It is still not definitely settled which superspace group describes the symmetry of the incommensurate phase of Rb_2ZnBr_4. Hogervorst and Helmholdt[5] have performed a structure determination on the basis of the (3 + 1)-dimensional space groups $Pcmn(00\gamma)(ss\bar{1})$, $Pc2_1n(00\gamma)(s\,\bar{1}\,\bar{1})$, and $P2_12_12_1(00\gamma)(\bar{1}\,\bar{1}\,1)$ and found the best—though doubt still exists—agreement with $Pcmn(00\gamma)(ss\bar{1})$; they claim, in agreement with measurements of Iizumi and Gesi,[9] that the actual structure is commensurate with $\gamma=\frac{5}{17}$, down to 10 K above T_c, although usage of the space group corresponding to that superstructure leads to less good results than when using the superspace group. A major difference between $Pcmn(00\gamma)(ss\bar{1})$ and the second-best candidate, $Pc2_1n(00\gamma)(s\,\bar{1}\,\bar{1})$, is that the former is centrosymmetric, while the latter is not. The commensurate superstructure with $\gamma=\frac{5}{17}$ would have symmetry $Pc2_1n$, which is not centrosymmetric and, in fact, would give the same predictions for the gyration tensor as given for phase III in Table II.

A general theory on the symmetry of tensors describing physical properties of structures with a superspace symmetry is not yet available despite the fact that, mathematically speaking, the restrictions imposed by a superspace group on tensor fields are well defined. The problem lies more in the fact that in the physical three-dimensional space, where the laws of physics are well known, the distinction between microscopic and macroscopic properties is less well defined than in the case of a normal crystal, because in three dimensions the unit cell of an incommensurate crystal is infinite and the notion of macroscopicity cannot be defined as involving length scales much larger than the elementary cell of the microscopic structure. In the (3 + d)-dimensional space, however, such a distinction is possible as the volume of the higher-dimensional unit cell is finite. The problem then arises of an appropriate extension of the physical laws to the higher-dimensional space. Such an extension is in principle possible, but not at all trivial. Here, the restrictions imposed by the superspace symmetry will be considered without extending the physical laws, but including more Fourier components than the constant one, as is done in the commensurate crystal case. An introductory approach to the problem can be found in Ref. 11. Some specific local tensorial properties, however, have already been examined within the context of superspace symmetry. For example, the electric-field-gradient (EFG) tensor in incommensurate phases has been studied by van Beest and Janner.[12] In the light of this treatment, the experimental data for the Rb EFG tensors and the Rb NMR

TABLE I. The different phases of Rb_2ZnBr_4. Given are the phase-transition temperatures (Ref. 5), the modulation wave vector ($\mathbf{q}=\gamma\mathbf{c}^*$), the space-group symmetry, and reported ferroelectric and antiferroelectric properties.

	Phase					
	VI	V	IV	III	II	I
Temp. (K)	<50	<77	<112	<190	<347	<753
γ	$\frac{1}{3}$	$\frac{1}{3}$	$\frac{1}{3}$	$\frac{1}{3}$	≈ 0.293	0 ($Z=4$)
Space group	$Pc11$(?)	$Pc11$(?)	$Pc2_1n$	$Pc2_1n$	$Pcmn(00\gamma)(ss\bar{1})$	$Pcmn$
Ferroel.	**b**	**b**	**b**	**b**		
Antiferroel.			**a**			

TABLE II. The various forms of the gyration tensor in the commensurate phases of Rb_2ZnBr_4 allowed by symmetry.

	Phase VI	Phase V	Phase IV	Phase III	Phase I
Gyration tensor	$\begin{pmatrix} 0 & g_{12} & g_{13} \\ g_{12} & 0 & 0 \\ g_{13} & 0 & 0 \end{pmatrix}$	$\begin{pmatrix} 0 & g_{12} & g_{13} \\ g_{12} & 0 & 0 \\ g_{13} & 0 & 0 \end{pmatrix}$	$\begin{pmatrix} 0 & 0 & g_{13} \\ 0 & 0 & 0 \\ g_{13} & 0 & 0 \end{pmatrix}$	$\begin{pmatrix} 0 & 0 & g_{13} \\ 0 & 0 & 0 \\ g_{13} & 0 & 0 \end{pmatrix}$	$\begin{pmatrix} 0 & 0 & 0 \\ 0 & 0 & 0 \\ 0 & 0 & 0 \end{pmatrix}$

line shape in both Rb_2ZnBr_4 and Rb_2ZnCl_4 are compatible with $Pcmn(00\gamma(ss\bar{1})$ as the superspace-group symmetry of the incommensurate phase in these compounds.[13] Hence, Rb_2ZnCl_4 would have a centrosymmetric incommensurate phase and consequently no optical activity. The latter conclusion, however, is in flagrant contradiction with the observations by Uesu and Kobayashi[14] and Sanctuary,[15] who found, though their results differ, a clear presence of optical activity in Rb_2ZnCl_4. This discrepancy does not mean that a superspace description is not appropriate, but it does show that care must be taken when considering the symmetry of different physical properties. In fact, the essential difference between NMR (EFG) and optical activity is the microscopic (macroscopic) nature of the phenomena. The NMR measurements mentioned above were performed on Rb sites, and they do not (or much less sensitively) probe the symmetry of the Zn and Br or Cl sites. In other words, the superspace-group symmetry element $m_y(s)$ can be present for the Rb atoms, but absent (or nearly so) for the other atoms. Optical activity, on the other hand, gives information regarding the symmetry on a much larger scale, of the order of the wavelength of the light used. There it probes, to a good approximation, the full symmetry of the crystal, though on a semimacroscopic scale. Care should be taken, however, in using the macroscopic limit, because for optical activity the wavelength of the light can essentially not be considered as infinite compared to the cell parameters, as the phenomenon is understood to be observable only for finite wavelength and, as already said, the cell parameters are themselves not all finite.[16] Furthermore, one has to realize that a centrosymmetric superspace group does not have the same structural consequences as a centrosymmetric space group. In the latter case the crystal has infinitely many inversion-symmetry points (at least one in each unit cell). That is also the case for the superspace unit cell, but not for the three-dimensional crystal, where (in general), at most, one inversion-symmetry point exists in the whole infinite crystal, the unit cell being of infinite size. In a finite crystal volume there is, therefore, strictly speaking, no center of inversion at all.

Instead of the superspace description, some authors use the approach which was introduced by Golovko and Levanyuk[17] in the case of $(NH_4)_2BeF_4$. They describe the dielectric function as a local property of the crystal, deviating from that determined by the average symmetry. Fousek and Kroupa[18] studied the particular case of Rb_2ZnCl_4 in this approach. The average symmetry is in the case of Rb_2ZnBr_4 the point group $m_x 2_y m_z$.

At this point it is worthwhile mentioning that the concept of local symmetry does not often provide the most exhaustive description. For example, in the NMR measurements, by adopting the same principle of a local crystal-field symmetry, a mirror operation m_y would not be involved, even not for Rb alone. So the local symmetry is not wrong, but does not fully take into account symmetry elements which possibly imply additional selection rules and is, furthermore, not always a well-defined concept. This is particularly the case when in a rational approximation, leading to a superstructure, the point group depends on the approximation adopted in the size of the unit cell.[19] Therefore, we think that it is advisable to take seriously into account the structural restrictions imposed on a microscopic scale by the superspace group in a way appropriate to the physical phenomenon considered. The present treatment of the dielectric and gyration tensor can serve as an illustration of how that can be done. Eventually, the correctness of this approach will have to be found in a comparison between experiment and theory.

III. OPTICAL SYMMETRY PROPERTIES IN THE INCOMMENSURATE PHASE

A. General

Our treatment of the symmetry properties of the dielectric tensor in an incommensurate phase is based on the superspace characterization of such a phase. We will specialize to the superspace-group symmetry of Rb_2ZnBr_4 and discuss the generalization to other members of the A_2BX_4 family members with the same superspace group $[Pcmn(00\gamma)(ss\bar{1})]$.[1] We will describe the optical properties of the crystal in terms of Fourier components of the tensor in question, which are relevant for the wave propagation of light and include the restrictions imposed by the superspace symmetry.

The basic equation is given by

$$\mathbf{D}(\mathbf{r},t)=\epsilon(\mathbf{r})\mathbf{E}(\mathbf{r},t)\ , \tag{1}$$

where we have taken a local dependence of the displacement field $\mathbf{D}$ on the electric field $\mathbf{E}$. We implicitly have assumed that we are far from resonances, i.e., the problem can be treated statically, with a time-independent dielectric tensor. This tensor $\epsilon(\mathbf{r})$ must have the symmetry of the crystal, and therefore Eq. (1) can be written as

$$\mathbf{D}(\mathbf{k})=\sum_{\mathbf{h}\in M^*}\epsilon(\mathbf{h})\mathbf{E}(\mathbf{k}-\mathbf{h})\ , \tag{2}$$

where M^* is the set of Fourier wave vectors occurring in the crystal structure. This implies in the present case that M^* is a Z module of rank 4, which is freely generated by $\mathbf{a}^*$, $\mathbf{b}^*$, $\mathbf{c}^*$ (spanning the reciprocal lattice Λ^* of the basic structure), and $\mathbf{q}=\gamma\mathbf{c}^*$ (the modulation wave vector). Note that all these vectors are defined in a three-dimensional space, so that up to now no embedding in a four-dimensional space is involved. In the description of light propagation in normal crystals, one realizes that the wave vectors for visible light are very small compared to any nonzero reciprocal-lattice vector, so Eq. (2) can very well be approximated by

$$\mathbf{D}(\mathbf{k})=\epsilon(\mathbf{0})\mathbf{E}(\mathbf{k}) , \tag{3}$$

where $\epsilon(\mathbf{0})$ can be viewed as a space-averaged dielectric tensor. This equation leads, together with Maxwell's equations ($\mathbf{n}=\mathbf{k}c/\omega$; ω is the frequency of the light),

$$\mathbf{D}(\mathbf{k})=n^2\mathbf{E}(\mathbf{k})-\mathbf{n}\mathbf{n}\cdot\mathbf{E}(\mathbf{k}) , \tag{4}$$

to the Fresnel equations, whose solutions specify the electric fields in the crystal and the refractive indices (n) in terms of the dielectric tensor elements $\epsilon_{ij}(0)$. In the case of an incommensurate crystal, however, periodicities are present with a considerably longer wavelength than in ordinary crystals. In principle, at least, M^* includes, because of the incommensurability between $\mathbf{q}$ and Λ^*, arbitrarily small Fourier wave vectors. Hence, one can expect that in these crystals nonzero reciprocal Z-module vectors also contribute substantially to the propagation of visible light. The description of the dielectric tensor as a microscopic entity, influenced by the relatively long waves, in a Landau-like approach, has been adopted by Golovko and Levanyuk[17] for $(NH_4)_2BeF_4$ and later by Fousek and Kroupa[18] for Rb_2ZnCl_4. It is therefore important to compare our results with those of the latter two authors. We will first solve the Fresnel equations taking into account additional Fourier elements of the dielectric tensor and afterwards also discuss the relations imposed by symmetry on the gyration tensor.

B. The dielectric tensor

The wave vectors in the rank-4 Z-module are specified by four integral indices (h,k,l,m), according to $\mathbf{h}=h\mathbf{a}^*+k\mathbf{b}^*+l\mathbf{c}^*+m\mathbf{q}$. In our case we take $\mathbf{q}=\gamma\mathbf{c}^*$ with γ irrational. it is then easy to see that the vectors $(0,0,l,m)$ for suitable choice of l and m are arbitrarily small. However, the larger the indices l or m, the smaller the structural information carried by the corresponding wave vector and, hence, the smaller its corresponding tensor $\epsilon(\mathbf{h})$ is expected to be. Therefore, we search for the smallest l and m indices, leading to wave vectors which are small compared to the dimensions of (say) the first Brillouin zone of the basic structure. An elegant method of finding l and m with these requirements is found in the continued-fraction expansion of γ. This approximation provides a unique series of fractions which converges to the irrational value of γ. For each step in the expansion, say l/m (l and m integer), the next step increases the value of both l and m. The reciprocal-lattice vector $(0,0,l,-m)$ therefore decreases in length, but with each step, normally speaking, also decreases in structural importance, as is typically observed in morphological and x-ray-diffraction investigations. We assume that such a decreasing contribution of Fourier components with higher indices is also met in the optical properties of modulated crystals. For $\gamma=0.293\ldots$, the resulting vectors are, in order of increasing length and descending importance, $(0,0,1,-3)$, $(0,0,2,-7)$, $(0,0,5,-17)$, $(0,0,12,-41)$, ... If we make a list of these vectors and determine their length, we find for the first three with the lowest indices (we use $|\mathbf{c}|=9.71$ Å)

$\mathbf{h}$	$2\pi/\lvert\mathbf{h}\rvert$ (Å)
$(0,0,1,-3)$	80.2
$(0,0,2,-7)$	190.4
$(0,0,5,-17)$	511.1

(5)

As long as we are in the sinusoidal regime of the modulation, i.e., not too far below the incommensurate phase transition, the structural importance of the higher harmonics can be neglected.

The next step will be to determine the form of the tensor $\epsilon(\mathbf{h})$ allowed by the superspace symmetry group [$G_s=Pcmn(00\gamma)(ss\bar{1})$ in our case]. The restrictions on the allowed Fourier components, as a result of the symmetry of the crystal, are analogous to what one finds when determining extinction rules for x-ray scattering. In the latter case, however, one searches for the Fourier components of a scalar field (the electron density), whereas in our case the tensor fields $\epsilon(\mathbf{r})$ and $\gamma(\mathbf{r})$ are relevant. As a result, it is possible to find that for a certain Fourier wave vector (say $\mathbf{h}$) one finds some tensor elements [$\epsilon_{ij}(\mathbf{h})$ or $\gamma_{ijk}(\mathbf{h})$] to be allowed for (nonzero), while the scalar field $\rho(\mathbf{h})$ is zero. Using G_s, the restrictions for the scalar field are [$\mathbf{h}=(h,k,l,m)$]

(h,k,l,m): no conditions ,
$(h,k,0,0)$: $h+k$ even ,
$(h,0,l,m)$: m even ,
$(0,k,l,m)$: 1 even .

These conditions imply, e.g., that the Fourier wave vectors in series (5) are not present in the scalar field; hence, for example $\mathbf{h}=(0,0,1,-3)$ has no structural contribution to the electron density, where only its higher harmonics of even order [like $(0,0,2,-6)$] are allowed. As we will see below, this wave vector, however, does allow for second-rank-tensor elements. This might seem contradictory, as one could expect that tensorial properties of a crystal are a result of the charge density in that crystal. On second thought, one realizes that the restrictions on the physical properties of a crystal are those imposed by the symmetry group of the Hamiltonian on the (many-body) wave function ψ. In an x-ray-diffraction experiment only the scalar charge density $|\psi|^2$ is observable within a fairly good approximation.[20] In the optical regime other restrictions and approximations apply. In the present paper no attempt is made to arrive at a microscopic understanding of the optical activity. A purely phenomenological point of view is adopted, based on the tensorial character of the quantity measured. It remains true that for those tensorial fields expressible in terms of

a scalar field (like the gradient field of a charge density) both the selection rules of the scalar and of the tensor fields apply. Such a restrictive assumption is not made here. We think that it is possible to have an allowed Fourier component in the dielectric (or gyration) tensor, while the corresponding electron density is absent. More generally, one can realize that in a multipole expansion of a given crystal structure it is possible to have Fourier wave vectors present for, e.g., the quadrupole, with a correspondingly zero charge density. Whether or not this more general situation occurs in Rb_2ZnBr_4 is a question of experimental facts.

Returning to our problem, we have to determine the tensor elements $\epsilon_{ij}(\mathbf{h})$, allowed by G_s. A general element g_s of G_s can be written as $\{R,R_I \mid \mathbf{t}_s\}$, with R the three-dimensional orthogonal transformation, R_I the corresponding internal element, and $\mathbf{t}_s$ a superspace translation.[2] The elements $\mathbf{h}$ of M^* can be embedded as reciprocal-lattice vectors $\mathbf{h}_s$ in the four-dimensional lattice Λ_4^*, with correspondingly the same integral components (h,k,l,m). The tensorial Fourier components are also embedded according to $\epsilon(\mathbf{h}_s)=\epsilon(\mathbf{h})$, and the invariance with respect to g_s is given by

$$\epsilon_{ij}(\mathbf{h})=R_{ik}R_{jl}\epsilon_{kl}(\mathbf{Rh})e^{i(\mathbf{R}_s\mathbf{h}_s)\cdot\mathbf{t}_s}\ , \tag{6}$$

where the Einstein summation convention (over repeated indices) is used. If we make a list of the scalar product $(\mathbf{R}_s\mathbf{h}_s)\cdot\mathbf{t}_s$ for the elements of G_s which are relevant, we find

g_s	$(\mathbf{R}_s\mathbf{h}_s)\cdot\mathbf{t}_s$
$\{c_x,1 \mid \frac{1}{2}0\frac{1}{2}\frac{1}{2}\}$	$\pi(-h+l+m)$
$\{m_y,1 \mid 0\frac{1}{2}0\frac{1}{2}\}$	$\pi(-k+m)$
$\{n_z,\bar{1} \mid \frac{1}{2}\frac{1}{2}\frac{1}{2}0\}$	$\pi(h+k-l)$
$\{\bar{1},\bar{1} \mid 0000\}$	0
$\{2_x,\bar{1} \mid \frac{1}{2}0\frac{1}{2}\frac{1}{2}\}$	$\pi(h-l-m)$
$\{2_y,\bar{1} \mid 0\frac{1}{2}0\frac{1}{2}\}$	$\pi(k-m)$
$\{2_z,1 \mid \frac{1}{2}\frac{1}{2}\frac{1}{2}0\}$	$\pi(-h-k+1)$
$\{1,1 \mid 0000\}$	0

For $\mathbf{h}=\mathbf{0}$, and hence $\mathbf{h}_s=\mathbf{0}$, Eq. (6) reduces to the symmetry condition for ordinary [three-dimensional (3D)] macroscopic tensors, thus bringing $\epsilon(\mathbf{0})$ to a diagonal form ($\epsilon_{ij}=\epsilon_i\delta_{ij}$) in our (orthorhombic) coordinate system.

For $\mathbf{h}\neq\mathbf{0}$, we find different results. One can specify l and m by their parity condition, thus finding (ϵ is diagonal; o=odd and e=even)

$$\begin{array}{cccc} l,m=0,0 & o,o & e,e & o,e \qquad\qquad e,o \\ \begin{bmatrix}\epsilon_1&0&0\\0&\epsilon_2&0\\0&0&\epsilon_3\end{bmatrix} & \begin{bmatrix}0&0&0\\0&0&\epsilon_4\\0&\epsilon_4&0\end{bmatrix} & \begin{bmatrix}\epsilon_6&0&0\\0&\epsilon_7&0\\0&0&\epsilon_8\end{bmatrix} & \begin{bmatrix}0&0&\epsilon_9\\0&0&0\\\epsilon_9&0&0\end{bmatrix}\begin{bmatrix}0&\epsilon_5&0\\\epsilon_5&0&0\\0&0&0\end{bmatrix} \end{array} . \tag{7}$$

Here we have introduced a short notation for the different tensor components. Note that $\epsilon(\mathbf{h})=\epsilon(-\mathbf{h})$ due to $\epsilon(\mathbf{r})$ being real in a lossless medium and because of the total inversion symmetry in G_s.

If we return to our basic equations (2), we could write these equations, restricting ourselves to (say) the first two wave vectors given in series (5) and higher harmonics. In order to limit the calculations, we will make the following approximation. Equations (2) will be solved in a two- and a three-Fourier-wave approximation, where one wave is given by $\mathbf{h}=\mathbf{0}$ and the other by one or two of such wave vectors. In the two-wave approximation, Eqs. (2) become (fields with wave vector $\mathbf{k}\pm2\mathbf{h}$ are neglected)

$$\begin{aligned}\mathbf{D}(\mathbf{k}-\mathbf{h})&=\epsilon\mathbf{E}(\mathbf{k}-\mathbf{h})+\epsilon(-\mathbf{h})\mathbf{E}(\mathbf{k})\ ,\\ \mathbf{D}(\mathbf{k})&=\epsilon(\mathbf{h})\mathbf{E}(\mathbf{k}-\mathbf{h})+\epsilon\mathbf{E}(\mathbf{k})+\epsilon(-\mathbf{h})\mathbf{E}(\mathbf{k}+\mathbf{h})\ ,\\ \mathbf{D}(\mathbf{k}+\mathbf{h})&=\epsilon(\mathbf{h})\mathbf{E}(\mathbf{k})+\epsilon\mathbf{E}(\mathbf{k}+\mathbf{h})\ .\end{aligned} \tag{8}$$

where we have written $\epsilon(\mathbf{0})=\epsilon$. Equations (8) combined with Maxwell's equations (4) give a set of equations for the Fourier components of the electric field, which in block-matrix form on the basis $\{\mathbf{E}(\mathbf{k}-\mathbf{h}),\mathbf{E}(\mathbf{k}),\mathbf{E}(\mathbf{k}+\mathbf{h})\}$ can be written as

$$\begin{bmatrix}\epsilon-\mathbf{F}(\mathbf{k}-\mathbf{h})&\epsilon(\mathbf{h})&\mathbf{0}\\ \epsilon(\mathbf{h})&\epsilon-\mathbf{F}(\mathbf{k})&\epsilon(\mathbf{h})\\ \mathbf{0}&\epsilon(\mathbf{h})&\epsilon-\mathbf{F}(\mathbf{k}+\mathbf{h})\end{bmatrix}\begin{bmatrix}\mathbf{E}(\mathbf{k}-\mathbf{h})\\ \mathbf{E}(\mathbf{k})\\ \mathbf{E}(\mathbf{k}+\mathbf{h})\end{bmatrix}=\begin{bmatrix}\mathbf{0}\\ \mathbf{0}\\ \mathbf{0}\end{bmatrix} . \tag{9}$$

In this equation

$$\mathbf{F}(\mathbf{k})=\begin{bmatrix}n_2^2+n_3^2&-n_1n_2&-n_1n_3\\ -n_1n_2&n_3^2+n_1^2&-n_2n_3\\ -n_1n_3&-n_2n_3&n_1^2+n_2^2\end{bmatrix} , \tag{10}$$

where $F(\mathbf{k}\pm\mathbf{h})$ is the matrix $\mathbf{F}(\mathbf{k})$, with $\mathbf{n}$ replaced by $\mathbf{n}\pm\mathbf{m}$. In this matrix, the n_i $(i=1,2,3)$ are the refractive indices for fields with wave vector $\mathbf{k}$ ($k=n\omega/c$). As no other frequencies are present in the crystal, we interpret the fields with wave vector $\mathbf{k}\pm\mathbf{h}$ as $\mathbf{k}\pm\mathbf{h}=(\mathbf{n}\pm\mathbf{m})\omega/c$. Note that the corresponding excitation can never be a solution of the normal Fresnel equations since $m^2\gg\epsilon_{ij}$. For $\lambda=630$ nm light, $n=1.65$; the corresponding value of m is $m\approx130$. The role of m is merely that of an alternative refractive index, which specifies the coupling of a light mode with wave vector $\mathbf{k}$ to the long-wavelength structural contributions to the dielectric constant. In other words, the normal modes for light propagation will have refractive indices which are predominantly determined by the Fresnel equations of the basic structure. There exists, however, a special case, for which $2\pi/|\mathbf{h}|$ is of the order of the wavelength of the light. That regime has been treated in a microscopic approach by van Beest,[21] but will be disregarded here. We will, nevertheless, discuss this regime in Sec. V B.

We first solved such a set of equations in a three Fourier-wave approximation, including $\mathbf{k}$, $\mathbf{k}\pm\mathbf{h}$, and $\mathbf{k}\pm2\mathbf{h}$, where $\mathbf{h}=(0,0,1,-3)$; this in order to be able to compare the results of our approach with those obtained

by Fousek and Kroupa.[18] In their approach, these authors found a diagonal contribution to ϵ, consisting of a position-independent part and a part which is modulated with wave vector 6q, where q is the modulation wave vector. Furthermore, they found a 3q-modulated contribution to ϵ_{23}. In fact, we find comparable results for $\epsilon(2\mathbf{h})$ and $\epsilon(\mathbf{h})$, respectively. The difference between their approach and ours is that they use the symmetry of the (approximate) commensurate phase ($\mathbf{q}=\frac{1}{3}\mathbf{c}^*$) and introduce a deviation via a space-dependent amplitude and phase of the modulation, where, as in our approach, we use the full symmetry of the incommensurate phase, albeit that we also neglect higher-order Fourier components. The results for the electric fields in our approximation are comparable to those of Fousek and Kroupa. Due to their commensurate approximation being limited to the vector $(0,0,\frac{1}{3})$ and its first harmonic, Fousek and Kroupa have also a different interpretation of the wave vector of the modulation, which is superimposed on the fields. In their approach the corresponding wavelengths are $|\mathbf{c}|=9.7$ Å and $|\mathbf{c}|/2$. In our approach the relevant wavelengths that one gets from the Z-module elements are much larger [cf. series (5)]. Obviously, the coupling between the light and the structural deformations will be larger when the wavelengths of both approach each other. Taking this and the results of the continued-fractions expansion (5) into account, we conclude that in the sinusoidal regime of the modulation, the first two Fourier components of structural importance are $\mathbf{h}_1=(0,0,1,-3)$ and $\mathbf{h}_2=(0,0,2,-7)$ and the contribution of $2\mathbf{h}_1$ can be neglected. Therefore we solved the Fresnel equations in the same way, now using $\mathbf{h}_1$ and $\mathbf{h}_2$, and found, for the three principal directions of propagation ($m_3=|\mathbf{h}_1|$ and $p_3=|\mathbf{h}_2|$), the following.

For $\mathbf{n}=(n_1,0,0)$,

$$E_1(\mathbf{r})=\left[\frac{2i\epsilon_4 n_1 m_3\sin(\mathbf{h}_1\cdot\mathbf{r})}{(n_1^2-\epsilon_3)(m_3^2-\epsilon_1)-n_1^2m_3^2}+\frac{2\epsilon_5(n_1^2-\epsilon_3)\cos(\mathbf{h}_2\cdot\mathbf{r})}{(n_1^2-\epsilon_3)(p_3^2-\epsilon_1)-n_1^2p_3^2}\right]E_2^0e^{i\mathbf{k}\cdot\mathbf{r}},$$

$$E_2(\mathbf{r})=E_2^0e^{i\mathbf{k}\cdot\mathbf{r}}, \tag{11}$$

$$E_3(\mathbf{r})=\left[\frac{2\epsilon_4(m_3^2-\epsilon_1)\cos(\mathbf{h}_1\cdot\mathbf{r})}{(n_1^2-\epsilon_3)(m_3^2-\epsilon_1)-n_1^2m_3^2}+\frac{2i\epsilon_5 n_1 p_3\sin(\mathbf{h}_2\cdot\mathbf{r})}{(n_1^2-\epsilon_3)(p_3^2-\epsilon_1)-n_1^2p_3^2}\right]E_2^0e^{i\mathbf{k}\cdot\mathbf{r}},$$

with

$$n_1^2=\epsilon_2+\frac{2\epsilon_4^2(m_3^2-\epsilon_1)}{(n_1^2-\epsilon_3)(m_3^2-\epsilon_1)-n_1^2m_3^2}+\frac{2\epsilon_5^2(n_1^2-\epsilon_3)}{(n_1^2-\epsilon_3)(p_3^2-\epsilon_1)-n_1^2p_3^2}\approx\epsilon_2-\frac{2\epsilon_4^2}{\epsilon_3}-\frac{2\epsilon_5^2(n_1^2-\epsilon_3)}{p_3^2\epsilon_3}\approx\epsilon_2-\frac{2\epsilon_4^2}{\epsilon_3}.$$

And

$$E_1(\mathbf{r})=0,\quad E_2(\mathbf{r})=\left[\frac{2\epsilon_4\cos(\mathbf{h}_1\cdot\mathbf{r})}{n_1^2+m_3^2-\epsilon_2}\right]E_3^0e^{i\mathbf{k}\cdot\mathbf{r}},\quad E_3(\mathbf{r})=E_3^0e^{i\mathbf{k}\cdot\mathbf{r}}, \tag{12}$$

with

$$n_1^2=\epsilon_3+\frac{2\epsilon_4^2}{n_1^2+m_3^2-\epsilon_2}\approx\epsilon_3+\frac{2\epsilon_4^2}{m_3^2}\approx\epsilon_3.$$

For $\mathbf{n}=(0,n_2,0)$,

$$E_1(\mathbf{r})=E_1^0e^{i\mathbf{k}\cdot\mathbf{r}},\quad E_2(\mathbf{r})=\left[\frac{2\epsilon_5(n_2^2-\epsilon_3)\cos(\mathbf{h}_2\cdot\mathbf{r})}{(n_2^2-\epsilon_3)(p_3^2-\epsilon_2)-n_2^2p_3^2}\right]E_1^0e^{i\mathbf{k}\cdot\mathbf{r}}, \tag{13}$$

$$E_3(\mathbf{r})=\left[\frac{2i\epsilon_5 n_2 p_3\sin(\mathbf{h}_2\cdot\mathbf{r})}{(n_2^2-\epsilon_3)(p_3^2-\epsilon_2)-n_2^2p_3^2}\right]E_1^0e^{i\mathbf{k}\cdot\mathbf{r}},$$

with

$$n_2^2=\epsilon_1+\frac{2\epsilon_5^2(n_2^2-\epsilon_3)}{(n_2^2-\epsilon_3)(p_3^2-\epsilon_2)-n_2^2p_3^2}\approx\epsilon_1-\frac{2\epsilon_5^2(n_2^2-\epsilon_3)}{p_3^2\epsilon_3}.$$

And

$$E_1(\mathbf{r})=0,\quad E_2(\mathbf{r})=\left[\frac{2\epsilon_4(n_2^2-\epsilon_3)\cos(\mathbf{h}_1\cdot\mathbf{r})}{(n_2^2-\epsilon_3)(m_3^2-\epsilon_2)-n_2^2m_3^2}\right]E_3^0e^{i\mathbf{k}\cdot\mathbf{r}}, \tag{14}$$

$$E_3(\mathbf{r})=\left[1+\frac{2i\epsilon_4 n_2 m_3\sin(\mathbf{h}_1\cdot\mathbf{r})}{(n_2^2-\epsilon_3)(m_3^2-\epsilon_2)-n_2^2m_3^2}\right]E_3^0e^{i\mathbf{k}\cdot\mathbf{r}},$$

with

$$n_2^2=\epsilon_3+\frac{2\epsilon_4^2(n_2^2-\epsilon_3)}{(n_2^2-\epsilon_3)(m_3^2-\epsilon_2)-n_2^2m_3^2}\approx\epsilon_3+\frac{2\epsilon_4^2(n_2^2-\epsilon_3)}{\epsilon_3m_3^2}.$$

For $\mathbf{n}=(0,0,n_3)$,

$$E_1(\mathbf{r})=E_1^0e^{i\mathbf{k}\cdot\mathbf{r}},\quad E_2(\mathbf{r})=\left[\frac{\epsilon_5}{(n_3+p_3)^2-\epsilon_2}e^{i\mathbf{h}_2\cdot\mathbf{r}}+\frac{\epsilon_5}{(n_3-p_3)^2-\epsilon_2}e^{-i\mathbf{h}_2\cdot\mathbf{r}}\right]E_1^0e^{i\mathbf{k}\cdot\mathbf{r}}, \tag{15}$$

$$E_3(\mathbf{r})=\left[-2\frac{\epsilon_4}{\epsilon_3}\cos(\mathbf{h}_1\cdot\mathbf{r})\right]E_1^0e^{i\mathbf{k}\cdot\mathbf{r}},$$

with

$$n_3^2=\epsilon_1+\frac{\epsilon_5^2}{(n_3+p_3)^2-\epsilon_2}+\frac{\epsilon_5^2}{(n_3-p_3)^2-\epsilon_2}$$
$$\approx\epsilon_1+2\frac{\epsilon_5^2}{p_3^2}\approx\epsilon_1 .$$

And

$$E_1(\mathbf{r})=\left[\frac{\epsilon_5}{(n_3+p_3)^2-\epsilon_1}e^{i\mathbf{h}_2\cdot\mathbf{r}}+\frac{\epsilon_5}{(n_3-p_3)^2-\epsilon_1}e^{i\mathbf{h}_2\cdot\mathbf{r}}\right]E_2^0e^{i\mathbf{k}\cdot\mathbf{r}} ,$$
$$E_2(\mathbf{r})=E_2^0e^{i\mathbf{k}\cdot\mathbf{r}} , \tag{16}$$
$$E_3(\mathbf{r})=\left[-2\frac{\epsilon_4}{\epsilon_3}\cos(\mathbf{h}_1\cdot\mathbf{r})\right]E_2^0e^{i\mathbf{k}\cdot\mathbf{r}} ,$$

with

$$n_3^2=\epsilon_2+\frac{\epsilon_5^2}{(n_3+p_3)^2-\epsilon_1}+\frac{\epsilon_5^2}{(n_3-p_3)^2-\epsilon_1}-2\frac{\epsilon_4}{\epsilon_3}$$
$$\approx\epsilon_2-2\frac{\epsilon_4}{\epsilon_3}+2\frac{\epsilon_5^2}{p_3^2}\approx\epsilon_2-2\frac{\epsilon_4}{\epsilon_3} .$$

In the different expressions for the refractive indices n_i, several approximations are given for which $m_3,p_3\gg n_i$ and $\epsilon_1,\epsilon_2,\epsilon_3\gg\epsilon_4,\epsilon_5$ are used. As a direct consequence, the refractive indices have values that differ only slightly from the ones in case of a macroscopic tensor. The solutions show a rocking and/or forward and/or backward movement of the electric field amplitude, depending on the position along **c** in the crystal. The magnitude of the additional field components is, however, very small. The electric fields and refractive indices at T_i approach continuously the solutions of the para phase, if we assume that the Fourier components $\epsilon(\mathbf{h})$ of the dielectric tensor can be written as a power series of the modulation amplitude. At the lock-in transition a symmetry change occurs, the mirror perpendicular to **y** being lost. Moreover, the wave vectors $(0,0,l,-m)$ lose their long-wavelength character, jumping to multiple values of $\mathbf{c}^*$. For intermediate temperatures, between the sinusoidal regime and the actual lock-in transition (the so-called discommensuration regime), the modulation involves more and more higher harmonics of the modulation wave with decreasing temperature. In this regime the temperature dependence of the wave vector also becomes stronger, but still can be written as $\mathbf{q}=[\frac{1}{3}-\delta(T)]\mathbf{c}^*$. The first vector resulting from the continued fractions expansion remains $(0,0,1,-3)$, while the following series of vectors rapidly changes with temperature. Thus, we expect the optical properties due to the modulation in the discommensuration regime to be mainly affected by this Fourier wave vector $(0,0,1,-3)$, with a gradual increase of the importance of its higher harmonics and relatively rapidly changing contributions as a function of temperature of the remaining vectors in the continued fractions expansion. These latter vectors can, in principle, have contributions to all dielectric tensor components. For the odd harmonics of $(0,0,1,-3)$, both l and m are odd, while for the even harmonics both are even. In series (7) we then find that the even harmonics only contribute to the diagonal tensor, which is the tensor form of the basic dielectric tensor, while all odd harmonics contribute to the element ϵ_4. Therefore, the optical properties are mainly determined by the tensor elements $\epsilon_1,\ldots,\epsilon_4$, resulting in a continuous behavior in the discommensuration regime, despite the strong temperature dependence of the modulation. At the lock-in transition one can expect a small discontinuity in the optical properties due to the jump of the wave vector to a commensurate value. In the lock-in phase the long-wavelength periodicities are no longer present, the vector $\mathbf{q}=\frac{1}{3}\mathbf{c}^*$ being the longest one. Because this length is small compared to the relevant vectors in the incommensurate phase, we expect the optical properties in the commensurate phase to be mainly determined by the macroscopic dielectric tensor $\epsilon(\mathbf{0})$, a normal constant (orthorhombic) diagonal tensor.

As was already stated by Fousek and Kroupa, the experimental observation of the small variations in the refractive indices is very difficult; they have to be isolated from the normal changes in refractive indices due to the thermal expansion of the cell.

C. Optical activity

In this section we will introduce the gyration tensor to the problem. For the description of optical activity, we refer the reader to Sommerfeld[16] and Born.[22] The effect of gyration is understood to be due to a nonlocal dependence of the displacement field $\mathbf{D}(\mathbf{r})$ on the electric field $\mathbf{E}(\mathbf{r})$. Again, the problem is assumed to be static. Because of this dependence, one can expect the long-wavelength structural properties of incommensurate phases to influence the gyration even more than the ordinary dielectric properties, as described in the preceding subsection. The basic material equation (1) is statically rewritten in a Taylor approximation as

$$\mathbf{D}(\mathbf{r})=\{\epsilon(\mathbf{r})+[\gamma(\mathbf{r})\nabla_{\mathbf{r}}]\}\mathbf{E}(\mathbf{r}) , \tag{17}$$

where the gyration tensor γ_{ijk} is a third-rank tensor, antisymmetric in its first two indices. Again, γ_{ijk} is a material tensor and therefore it has the symmetry of the crystal, so that we can rewrite the Fourier transform of Eq. (17) as

$$\mathbf{D}(\mathbf{k})=\sum_{\mathbf{h}\in M^*}\{\epsilon(\mathbf{h})+[i\gamma(\mathbf{h})(\mathbf{k}-\mathbf{h})]\}\mathbf{E}(\mathbf{k}-\mathbf{h}) , \tag{18}$$

where the differentiation has been performed. As $\gamma_{ijk}(\mathbf{r})=-\gamma_{ijk}(-\mathbf{r})$ and $\gamma_{ijk}(\mathbf{r})$ is a real tensor, one has $\gamma_{ijk}(\mathbf{h})=-\gamma_{ijk}(-\mathbf{h})$. Before determining its form, we briefly describe the contraction of γ to a vector $\gamma^{(\mathbf{k})}$, the so-called gyration vector, and a second-rank pseudotensor g_{ij}, which are normally used to describe the gyration properties of crystals. First, a second-rank antisymmetrical tensor is introduced by

$$\gamma_{ij}^{(\mathbf{k})}(\mathbf{h})=\gamma_{ijl}(\mathbf{h})\mathbf{k}_l . \tag{19}$$

The gyration vector is then written as

$$\gamma_i^{(\mathbf{k})}(\mathbf{h})=\tfrac{1}{2}e_{ijl}\gamma_{jl}^{(\mathbf{k})}(\mathbf{h}) , \tag{20}$$

where $e_{ijl}=\frac{1}{2}(i-j)(j-l)(l-i)$, resulting in

$$\mathbf{D}(\mathbf{k})=\sum_{\mathbf{h}\in\Lambda_4^*}[\epsilon(\mathbf{h})\mathbf{E}(\mathbf{k}-\mathbf{h})-i\boldsymbol{\gamma}^{(\mathbf{k}-\mathbf{h})}(\mathbf{h})\times\mathbf{E}(\mathbf{k}-\mathbf{h})] . \tag{21}$$

The effect of optical activity is now observed as a rotation of the polarization around the wave normal $\mathbf{k}$ of the light, whenever $\mathbf{k}\cdot\boldsymbol{\gamma}^{(\mathbf{k})}(\mathbf{r})\neq 0$, the effect of the birefringence on the optical activity being neglected. A more common notation for the optical activity is in terms of a second-rank-real pseudotensor g_{ij}, which can be defined from

$$\gamma_i=-g_{ij}k_j . \tag{22}$$

The symmetry properties for the g_{ij} can be found, e.g., in Nye.[10]

Returning to Eq. (17), we will determine the form of γ_{ijk}, using the superspace symmetry of the crystal. The symmetry condition for $\gamma_{ijk}(\mathbf{h})$ now reads

$$\gamma_{ijk}(\mathbf{h})=R_{im}R_{jn}R_{kp}\gamma_{mnp}(\mathbf{R}\mathbf{h})e^{i(\mathbf{R}_s\mathbf{h}_s)\cdot\mathbf{t}_s} . \tag{23}$$

For $\mathbf{h}=\mathbf{0}$ using the elements of G_s, this leads to $\gamma_{ijk}(0)=0$, predicting no optical activity within this approximation. The observed effect is thus due to the modulation-dependent ($m\neq 0$) wave vectors, and again we restrict our considerations to those given in series (5). In order to obtain results which can directly be related to the experimental directions of the wave normals, we give the gyration vectors for different directions of $\mathbf{k}$, for all parity conditions of l,m in $\mathbf{h}=(0,0,l,m)$, in Table III. If we restrict ourselves to the first Fourier wave vector of important [$\mathbf{h}=(0,0,1,-3)$], we find in this table, without specifying the exact form of the fields (which still need further investigation), that optical activity can only be present for the direction $\mathbf{k}=(k_1,0,k_3)$, with $k_1\neq 0$ and $k_3\neq 0$. All other directions for $\mathbf{k}$ are perpendicular to the corresponding gyration vector. Physically, this is understood as follows. Only the fields for $\mathbf{k}=(k_1,0,k_3)$ can show gyrational effects due to the coupling with fields with wave vector $\mathbf{k}\pm(0,0,1,-3)$. If we include the next Fourier component $\mathbf{h}_2=(0,0,2,-7)$, we find that rotation is, in principle, possible for all directions of $\mathbf{k}$. The appearance of a net observable rotation depends on other conditions as well, which are not yet fully explored. Some of the expected ones are presented in Sec. V.

IV. EXPERIMENT

A. HAUP polarimeter

The measurements were performed by means of a HAUP polarimeter as described by Kobayashi *et al.*[4] The light source was a He-Ne laser (632.8 nm); the extinction ratio of the polarizer and analyzer were specified to be 10^{-6}; the resolution of the stepping-motor-driven Nicol polarizers was approximately 0.001°. For all measurements the polarizers were rotated both from $-0.5°$ to $+0.5°$ with respect to their zero positions, with intervals of 0.05°. For each position the intensity was measured with a photon-counting system for a period of 1 s and

TABLE III. The form of the gyration vectors $\boldsymbol{\gamma}^{(\mathbf{k})}(\mathbf{h})$ for different wave vectors ($\mathbf{k}$) of the light and all parity conditions of l and m in $\mathbf{h}=(0,0,l,m)$; e denotes even, o denotes odd. The entries are given in terms of the gyration tensor element γ_{ijk} [see Eqs. (19) and (20)].

	l,m				
k	0,0	*o,o*	*e,e*	*o,e*	*e,o*
(1,0,0)	$\begin{bmatrix}0\\0\\0\end{bmatrix}$	$\begin{bmatrix}0\\0\\\gamma_{121}\end{bmatrix}$	$\begin{bmatrix}0\\-\gamma_{131}\\0\end{bmatrix}$	$\begin{bmatrix}0\\0\\0\end{bmatrix}$	$\begin{bmatrix}\gamma_{231}\\0\\0\end{bmatrix}$
(0,1,0)	$\begin{bmatrix}0\\0\\0\end{bmatrix}$	$\begin{bmatrix}0\\0\\0\end{bmatrix}$	$\begin{bmatrix}\gamma_{232}\\0\\0\end{bmatrix}$	$\begin{bmatrix}0\\0\\\gamma_{122}\end{bmatrix}$	$\begin{bmatrix}0\\-\gamma_{132}\\0\end{bmatrix}$
(0,0,1)	$\begin{bmatrix}0\\0\\0\end{bmatrix}$	$\begin{bmatrix}\gamma_{233}\\0\\0\end{bmatrix}$	$\begin{bmatrix}0\\0\\0\end{bmatrix}$	$\begin{bmatrix}0\\-\gamma_{133}\\0\end{bmatrix}$	$\begin{bmatrix}0\\0\\\gamma_{123}\end{bmatrix}$
(1,1,0)	$\begin{bmatrix}0\\0\\0\end{bmatrix}$	$\begin{bmatrix}0\\0\\\gamma_{121}\end{bmatrix}$	$\begin{bmatrix}\gamma_{232}\\-\gamma_{131}\\0\end{bmatrix}$	$\begin{bmatrix}0\\0\\\gamma_{122}\end{bmatrix}$	$\begin{bmatrix}\gamma_{231}\\-\gamma_{132}\\0\end{bmatrix}$
(0,1,1)	$\begin{bmatrix}0\\0\\0\end{bmatrix}$	$\begin{bmatrix}\gamma_{233}\\0\\0\end{bmatrix}$	$\begin{bmatrix}\gamma_{232}\\0\\0\end{bmatrix}$	$\begin{bmatrix}0\\-\gamma_{133}\\\gamma_{122}\end{bmatrix}$	$\begin{bmatrix}0\\-\gamma_{132}\\\gamma_{123}\end{bmatrix}$
(1,0,1)	$\begin{bmatrix}0\\0\\0\end{bmatrix}$	$\begin{bmatrix}\gamma_{233}\\0\\\gamma_{121}\end{bmatrix}$	$\begin{bmatrix}0\\-\gamma_{131}\\0\end{bmatrix}$	$\begin{bmatrix}0\\-\gamma_{133}\\0\end{bmatrix}$	$\begin{bmatrix}\gamma_{231}\\0\\\gamma_{123}\end{bmatrix}$

corrected with a reference signal to take care of drift in the laser output power.

B. Temperature control

The sample was mounted on a cold or hot finger with as little stress as possible to avoid induced optical activity. Thermal contact was improved with thermal paste. The sample was completely surrounded by a copper radiation shield at the samples temperature (except for two small holes for the transmitted light). Temperature was controlled with a heater in the cold or hot finger and a Pt-100 resistor as a thermometer. For temperatures below room temperature the sample was cooled with an additional N_2 or He flow through the cold finger. A second Pt-100 resistor, mounted in the sample holder, was used to measure the temperature of the sample. The temperature stability was always better than ± 0.01 K and the absolute error was estimated to be less than ± 1 K.

C. Samples

The samples used were grown with a modified Bridgman technique. Starting material was obtained from crystals grown from an aquaeous solution containing RbBr and $ZnBr_2$ in the molar ratio 2:1, slightly acidified with concentrated HCl to improve growth. The growing rate from the melt was 0.6 mm/h. The thus-obtained transparent crystal was cleaved perpendicular to **a**, oriented further with a polarizing microscope, and sawed with a string saw. The faces to be used for the experiment were polished to a local flatness of about 1 μm. All samples were measured no longer than 1 d after they were polished in order to avoid contamination of the surfaces due to the hygroscopic nature of the material.

The off-diagonal gyration tensor elements were measured along the bisectors of the corresponding axes with the exception of g_{13}, which was measured along a direction tilted over 15° from the bisector towards the **a** axis, because the optical axis turned out to be approximately along this bisector (at room temperature). All three samples used were obtained from the same melt growth. The samples are denoted as $\mathcal{S}_{ij}$, where the indices indicate the orientation of the cut as adapted to the measurement of the tensor element g_{ij}. Their dimensions were $\mathcal{S}_{11}$, $\approx 5\times 8$ mm^2 and 1.65 mm thick; $\mathcal{S}_{12}$, $\approx 8\times 12$ mm^2 and 1.95 mm thick; and $\mathcal{S}_{13}$, $\approx 8\times 12$ mm^2 and 1.01 mm thick.

D. Results and evaluation

For the evaluation of the results, we used the following procedure. All data were fitted to the following formula describing the measured intensity (Γ) in terms of the polarizer position (θ) and the analyzer position (Λ):

$$\Gamma=\Gamma_0\{A_0+[\chi-\cos(\Delta/2)(\theta-\Lambda)]^2 +[\sin(\Delta/2)(\theta+\Lambda)]^2\}\ , \tag{24}$$

where Γ_0 is the incoming intensity, A_0 a background intensity due to scattering,

$$\chi=[(\gamma-2k)\sin(\Delta/2)+\delta\Lambda\cos(\Delta/2)]$$

with $\gamma=p-a$ the difference in ellipticity of the polarizer and the analyzer, Δ the phase difference for the light due to the sample, $\delta\Lambda$ a measure for the misalignment of the sample, and $k\approx g/2\Delta\bar{n}$, where g is the optical activity and $\bar{n}$ is the effective refractive index. This formula is in essence the same as that given by Kobyashi[4] and is derived elsewhere.[23] The procedure suggested by Kobayashi,[4] which fits the results to Y ($Y=\theta-\Lambda$) and uses in a second fit to θ the first-fit results, was not adequate in our case because the data points were quite scattered, mainly due to problems with the mechanical interface between the stepping motors and the Nicols polarizer. Therefore we adopted this procedure only to obtain starting values for the parameters used in another fit procedure, which fits the data with respect to both θ and Λ simultaneously. Thus we obtained values for $|\cos(\Delta/2)|$, χ, A_0, and Γ_0 as a function of temperature. One drawback of the HAUP technique is the fact that one always needs to know a value of Δ and the sign of $\partial\Delta/\partial T$ at a certain temperature because the measurement gives only values for $|\cos(\Delta/2)|$. Therefore the birefringence was measured for all three samples at room temperature. This was done by measuring very accurately the three refractive indices with an Abbe refractometer, using an interference filter to obtain light with a wavelength of 634 nm. The results were ($T=297\pm 1$ K)

$$n_a=1.6448\pm 0.0002\ ,$$

$$n_b=1.6518\pm 0.0004\ ,$$

$$n_c=1.6573\pm 0.0002\ .$$

The refractive indices were also measured for other wave lengths; at 514.5 nm we found

$$n_a=1.659\ ,$$

$$n_b=1.666\ ,$$

$$n_c=1.672\ .$$

These values are systematically smaller (0.3–0.5 %) than those obtained by Horikx,[24] but consistent with the data of Kusto *et al.*[25] ($\lambda=589$ nm). The value for the birefringence was calculated for all three samples used ($\lambda=634$ nm; Δn_{ij} is the birefringence as observed for light traveling along a direction perpendicular to the sample denoted by $\mathcal{S}_{ij}$):

$$\Delta n_{11}=(5.5\pm 0.5)\times 10^{-3}\ ,$$

$$\Delta n_{12}=(9.0\pm 0.5)\times 10^{-3}\ ,$$

$$\Delta n_{13}=(2.3\pm 0.5)\times 10^{-3}\ .$$

These values were used to extract the correct values for the birefringence as a function of temperature from the fit results for $|\cos(\Delta/2)|$. The sign of the slope for this function was assumed to be the same as for Rb_2ZnCl_4 and taken from Ref. 15. Both γ and $\delta\Lambda$ are assumed to be independent of temperature. The value for $\delta\Lambda$ was obtained by averaging all values of $\chi/\cos(\Delta/2)$ with $\sin^2(\Delta/2)<0.5$, and the value γ by averaging all values of $[\chi-\delta\Lambda\cos(\Delta/2)]/\sin(\Delta/2)$ in the paraelectric phase,

where $k=0$. In this way, $g=2k\,\Delta\bar{n}$ was obtained as a function of temperature. The results for the birefringence are given in Figs. 1(a)–1(c); those for the optical activity in Figs. 2(a)–2(c).

V. DISCUSSION

A. Rb_2ZnBr_4

We will first concentrate on the results for the birefringence as a function of temperature. At this point we have to emphasize that the small jumps in the birefringence as predicted in Sec. III cannot be observed by means of HAUP. Very precise differential measurements of the birefringence, however, can reveal those jumps.[26] Our comparisons with Rb_2ZnCl_4 refer to Sanctuary.[15]

For $\mathcal{S}_{11}$ we see in Fig. 1(a) that the value of Δn_{yz} increases almost linearly with increasing temperature within the incommensurate phase and the lock-in phase (phase III). There is no clear change at the lock-in transition temperature (T_c). Above T_i the slope diminishes; the same behavior can be seen for temperatures in phases IV and V. The behavior in the neighborhood of T_i is confirmed by the measurements of Kusto *et al.*,[25] although they found a value of $\Delta n_{11}=4.5\times10^{-3}$ at 300 K for $\lambda=632.8$ nm, whereas we find $\Delta n_{11}=5.3\times10^{-3}$.

For $\mathcal{S}_{12}$, the birefringence $(\Delta n_{zx}-\frac{1}{2}\Delta n_{yx})$ shows the same behavior as for $\mathcal{S}_{11}$, only the slope in the para phase is in this case almost the same as in the incommensurate phase. At T_c a very small change in the slope is present. In the neighborhood of the transition to phase V, the sign of the slope changes. In phase V the slope seems to be constant again, while in the intermediate phase, IV, the behavior is far from linear.

For $\mathcal{S}_{13}$, again an analogous behavior is observed, although no measurements were done in phase V. The change in slope at T_i is more pronounced than for $\mathcal{S}_{12}$ and in the neighborhood of T_c, again, a very small change in slope can be seen. In all three cases the slope is—in the incommensurate and lock-in phase—approximately $(0.5-1)\times10^{-5}\ \mathrm{K}^{-1}$, which is comparable with the result found for Rb_2ZnCl_4. The changes in the neighborhood of the transition temperatures to phases IV and V do not coincide with the reported temperatures (112 and 77 K). In fact, at 112 K only small gradual changes are observed, which is in agreement with the reported[5] small differences between phases III and IV. The change in the sign of the slope in the case of $\mathcal{S}_{12}$ is probably related to the phase transition to phase V, indicating a higher transition temperature in our sample ($\approx$85 K). The highest temperature reported for this transition is 80 K.[8]

Next we will devote our attention to the optical activity. As was mentioned before, one can see in Fig. 2 that the data points scatter quite a lot. Nevertheless, we can draw the following conclusions.

The gyration coefficient g_{11} stays small ($<1\times10^{-5}$) for all temperatures measured. The small gradual increase with decreasing temperature is probably due to a small change of $\delta\Lambda$ with temperature. Except for phase V, the

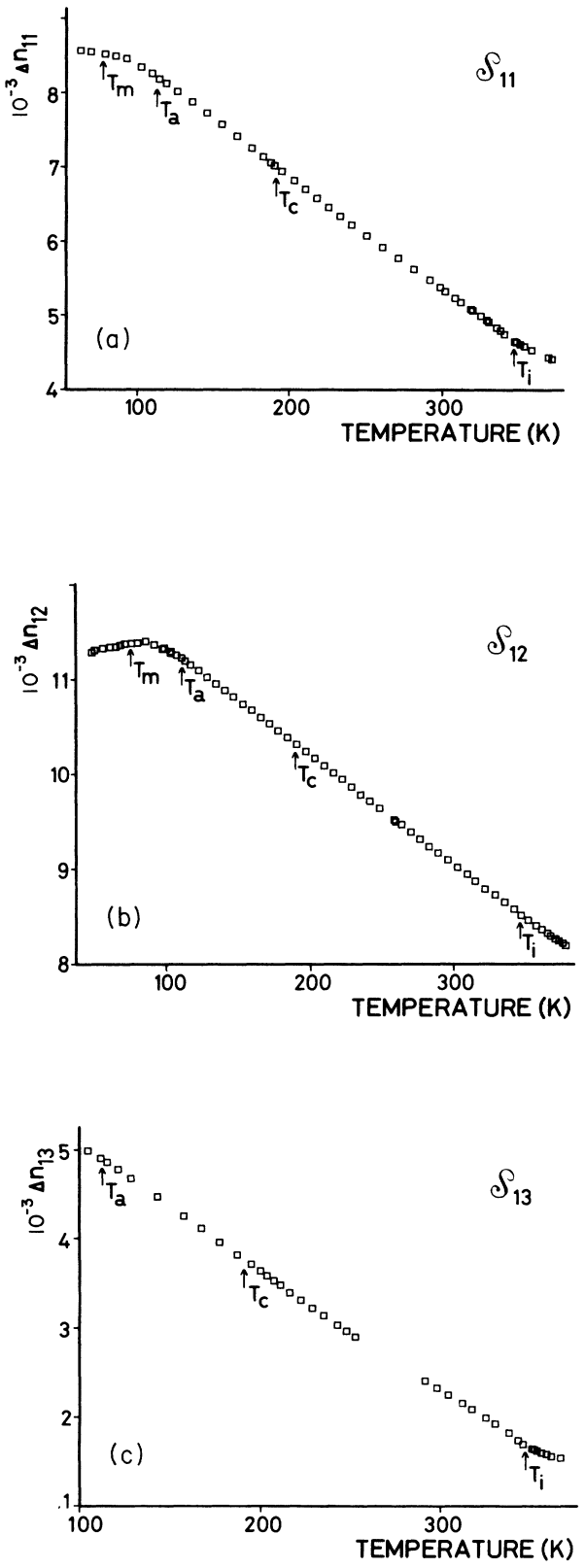

FIG. 1. (a) The birefringence as a function of temperature for $\mathcal{S}_{11}$ (Δn_{yz}). Indicated are the different phase transitions. (b) The birefringence as a function of temperature for $\mathcal{S}_{12}$ ($\Delta n_{zx}-\frac{1}{2}\Delta n_{yx}$). Indicated are the different phase transitions. (c) The birefringence as a function of temperature for $\mathcal{S}_{13}$ ($\Delta n_{xy}-\frac{3}{4}\Delta n_{xz}$). Indicated are the different phase transitions.

same holds for g_{12} ($<1\times10^{-5}$). Below approximately 77 K, g_{12} systematically increases.

A different behavior is observed for g_{13}. This coefficient increases considerably at T_i and continues to do so down to the lowest temperature measured (≈100 K). At T_c, the value for g_{13} is approximately 2.3×10^{-5}; cf. Rb_2ZnCl_4, where $g_{13}(T_c)\approx4.0\times10^{-5}$. The slope is approximately -1.0×10^{-7} K^{-1}. (In Rb_2ZnCl_4, -4.5×10^{-7} K^{-1}).

If we compare these results with the predictions for the commensurate phases given in Sec. II, we see that both values are consistent. The value of g_{13} increases down to 100 K, indicating that the order parameter responsible for the optical activity does the same. The nonzero value for g_{12} in phase V indicates that the symmetry element n_z of phases III and IV is indeed lost, resulting in the point-group symmetry m_x, consistent with the predicted space group $Pc11$. If we compare this result with Rb_2ZnCl_4, where a low-temperature phase transition to a monoclinic phase (probably $Pc11$) is also found,[27] we observe that the phase-transition temperatures in the two compounds do not differ much [$T_i=303$ K (437 K), $T_c=192$ K (190 K), and $T_m=75$ K (77 K) for Rb_2ZnCl_4 (Rb_2ZnBr_4)]. Unfortunately, the optical activity in Rb_2ZnCl_4 has only been determined for g_{13} and only down to 150 K.

The nonzero value of g_{13} in the incommensurate phase is in agreement with the predictions of Sec. III. Moreover, the fact the g_{11} and g_{12} stay relatively small indicates that in Rb_2ZnBr_4 the contributions to the optical activity of the Fourier component $\mathbf{h}=(0,0,1,-3)$ are far more important then those of the next one [cf. series (5)].

The fact that g_{13} has a nonzero value in the incommensurate phase was also observed in Rb_2ZnCl_4; the only difference is that Sanctuary[15] finds a nonzero value starting about 50 K below T_i, while Uesu *et al.*[14] find (as we do for Rb_2ZnBr_4) a nonzero value immediately below T_i. On the other hand, in both Sanctuary's and our case g_{13} increases monotonically (almost linearly) with decreasing temperature, while Uesu and Kobayashi report a tendency for the gyration to go to zero at the lock-in transition and increase again upon entering the lock-in phase. Kobayashi *et al.* also reported this behavior for $[N(CH_3)_4]_2ZnCl_4$, for which they found another result, where g_{13} does not go to zero at T_c, but rather jumps to a larger value, in later measurements.[4] Therefore the effect at T_c seems to depend on the sample. This is consistent with the view of Saito *et al.*[28] that domain walls (solitons) represented by discommensuration regions between nearly commensurate domains have an influence on the gyration tensor. Pinning, due to defects, enhance these effects. This situation can also be described within the present approach, by including higher harmonics in the Fourier components considered. On the other hand, our measurements show very little variation with temperature within the full incommensurate phase, so that no appreciable difference is observed between the typical sinusoidal regime (near the incommensurate phase-transition temperature) and the discommensuration regime, near the lock-in phase. This fact can be considered to support the present approach in terms of relevant

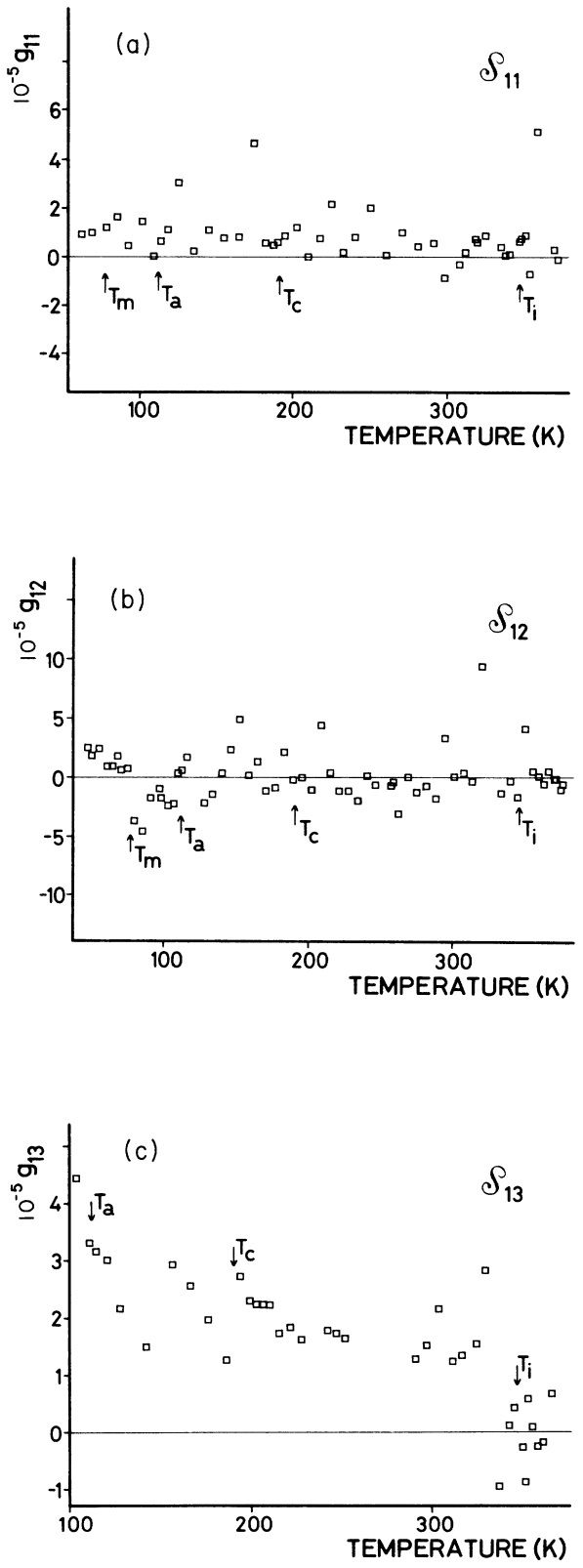

FIG. 2. (a) The gyration tensor element (g_{11}) as a function of temperature for $\mathcal{S}_{11}$. Indicated are the different phase transitions. (b) The gyration tensor element (g_{12}) as a function of temperature for $\mathcal{S}_{12}$. Indicated are the different phase transitions. (c) The gyration tensor element (g_{13}) as a function of temperature for $\mathcal{S}_{13}$. Indicated are the different phase transitions.

nonzero Fourier waves. There is a possibility for a net rotation, despite the periodic spatial dependence of the gyration tensor considered, because of the same periodic properties of the dielectric tensor, which influence the stabilization of layers relevant for domains, defects and/or morphologically stable faces. Accordingly, not all gyration amplitudes are equally probably, leading to a net rotation which is possibly crystal dependent.

B. Other A_2BX_4 compounds

As the incommensurate phases of all members of the A_2BX_4 family of dielectrics studied up to now are believed to have as their symmetry the superspace group $Pcmn(00\gamma)(ss\bar{1})$,[1] a generalization of our results for Rb_2ZnBr_4 to the other members is appealing. This generalization, however, has to take into account the different continued fractions expansions of the modulation parameters γ, which are not the same for different compounds and can be temperature dependent. The Fourier wave vector corresponding to the first term in this expansion is not necessarily $(0,0,1,-3)$ or more general $(0,0,l,m)$ with both l and m odd. In Rb_2ZnBr_4 the modulation wave vector is independent of temperature for a large temperature range of the incommensurate phase; approximately 10 K above the lock-in phase transition it starts to deviate from this constant value.

In Rb_2ZnCl_4 a comparable behavior is observed. The value of the modulation wave vector is fairly constant ($\gamma=0.31$).[29] Its continued fractions expansion starts with $\frac{1}{3}$, the next approximation being already $\frac{11}{34}$. A few degrees kelvin above T_c (190 K), the value of γ is approximately 0.32, with $\frac{1}{3}$ and $\frac{8}{25}$ as its first two fractional approximations. This example shows that the contributions of the first Fourier wave vector $(0,0,1,-3)$ are expected to be the most prominent ones through the incommensurate phase. Of course, the effect of higher harmonics, playing a more substantial role in the neighborhood of the lock-in transition, can change this situation.

In $[N(CH_3)_4]_2ZnCl_4$ (TMAZC), however, the modulation wave vector is much more temperature dependent. Furthermore, its continued fractions expansion (of $\gamma=0.42$ at $T=290$ K) provides as first approximation $\mathbf{h}=(0,0,2,-5)$, thus predicting (see Table III) the possibility of optical activity for every direction of $\mathbf{k}$. Unfortunately, the gyration effect in this compound has only been studied for the direction $\mathbf{k}=(k_1,0,k_3)$,[4] where a small (100 times smaller as compared to Rb_2ZnBr_4) effect was observed. Nevertheless, it would be interesting to measure the optical activity for other directions in TMAZC. One has to note, however, that the relevant γ_{ijk} can differ in magnitude. On the other hand, Table III, together with Eq. (22), shows that if g_{33} is observable (which is experimentally verified), also g_{11} or g_{33} and probably g_{12} or g_{23} should be observable and have the same order of magnitude as g_{13}. The change of γ as a function of temperature, however, makes it more difficult to find the appropriate continued fractions expansion. We realize that this variation of γ with temperature implies, within our model, that different tensor components get larger and smaller in value as the temperature is lowered. The correct interpretation and physical consequences of this behavior will be disregarded here, but will certainly be a topic of future work.

As was mentioned before, the Fourier wave vectors with lengths comparable to the wavelength of the light in the crystal (approximately 380 nm in our case) could provide for a kind of resonant behavior. The gyration effect is expected to be much larger in the corresponding regime, which is often met in cholesteric liquid crystals.[30] As long as the deviation δ of the incommensurate wave vector from its commensurate value is not too small, these "resonant" wave vectors will have very high indices l and m. In the case of Rb_2ZnBr_4 the value $\gamma=0.2930$, which is constant for a large temperature interval, would imply vectors like $(0,0,17,-58)$ and $(0,0,46,-157)$ with lengths of approximately 162 and 971 nm, respectively. On the other hand, the experimental error is $\gamma=0.293\pm0.001$ and therefore one cannot say much about the relevance of these large-index Fourier components, as e.g., $\gamma=0.2940$ would imply that the vector $(0,0,5,-17)$ already has a length of 486 nm. In other words, high-index Fourier wave vectors can be relevant for an observed gyration effect, but one cannot deduce from the experimentally observed value of the incommensurate wave vector which indices are important. Moreover, a temperature dependence of the wave vector is most prominently effective in these high-index vectors, resulting again in a rather wild change in relevance of the corresponding optical Fourier tensors as a function of temperature. The first three fractions in the continued expansion ($\frac{1}{3}$, $\frac{2}{7}$, and $\frac{5}{17}$) are, however, present for all values 0.293 ± 0.001.

VI. CONCLUSIONS

We have measured the gyration coefficients g_{11}, g_{12}, and g_{13} as well as the birefringence of the corresponding directions in Rb_2ZnBr_4 in its paraelectric phase, the incommensurate phase, and the lock-in phase. g_{11} and g_{12} were also determined in the low-temperature monoclinic phase.

As far as the commensurate phases are concerned, the expected gyration effects, on symmetry grounds, are in agreement with the experimental results. The phase transition at T_a (112 K) between two orthorhombic phases with the same symmetry has no observable effects on the optical activity, nor on the birefringence. The existence of a low-temperature monoclinic phase ($T<77$ K) is confirmed. The lock-in transition has a very small influence on the optical properties. The linear dependence of the birefringence on temperature changes its slope slightly at T_c.

In the incommensurate phase optical activity was observed only for g_{13}. In order to explain the observed effect, we developed a phenomenological theory on the basis of the superspace symmetry of this phase. In this theory, the dielectric tensor and the gyration tensor are semimicroscopic (local) entities. Note that this is commonly also done for x-ray diffraction in the kinematic approximation. The Fourier components $\epsilon(\mathbf{h})$ and $\gamma(\mathbf{h})$ have decreasing contributions to the propagation of light,

with increasing $\mathbf{h}$, but also with increasing integral components of $\mathbf{h}$ as elements of a fourth-rank Z module. The choice of the relevant Fourier components must be based on phenomenological grounds as long as a microscopic theory is not available. For normal crystals the smallest nonzero Fourier wave vector is a reciprocal-lattice vector whose wavelength is very small compared to the wavelength of the light used. In the incommensurate structure, however, relatively long-wavelength structural information is present in the Fourier expansion, which can contribute substantially to the spatial variation expressed by $\epsilon(\mathbf{r})$ and $\gamma(\mathbf{r})$. The allowed Fourier components and their tensor forms follow from the superspace symmetry, the selection rules being, of course, dependent on the rank. We used the first three Fourier components expected to be of importance in Rb_2ZnBr_4 to find the electric fields in the absence of optical activity, for the three principal directions of propagation. In the case of optical activity, we determined the symmetry of the different Fourier components of the gyration tensor and used these results to explain the observed effect in the incommensurate phase.

Finally, a generalization of the theory to other incommensurate structures has been discussed.

ACKNOWLEDGMENTS

The measurements were performed in the research group of Professor Dr. P. Günter, Laboratorium für Festkörperphysik, Eidgenössische Technische Hochschule–Zürich, Switzerland. We gratefully acknowledge the kind hospitality and, in particular, would like to thank Dr. Herbert Looser and Mr. J. Hajfler for their contributions. The valuable critical remarks by Professor Dr. F. Tuinstra have been greatly appreciated and have helped the authors arrive at a more explicit formulation of their point of view. Stimulating discussions with Dr. T. Janssen are also acknowledged. This work is part of the research program of the Stichting voor Fundamenteel Onderzoek der Materie (Foundation for Fundamental Research on Matter) and was made possible by financial support from the Nederlandse Organisatie voor Zuiver-Wetenschappelijk Onderzoek (Netherlands Organization for the Advancement of Pure Research).

[1]A. C. R. Hogervorst, Ph.D. thesis, University of Delft, 1986.

[2]A. Janner and T. Janssen, Acta Crystallogr. Sect. A **33**, 493 (1977); Phys. Rev. B **15**, 643 (1977).

[3]T. Janssen and A. Janner, Adv. Phys. **36**, 519 (1987).

[4]J. Kobayashi, H. Kumomi, and K. Saito, J. Appl. Crystallogr. **19**, 377 (1986), and references therein.

[5]A. C. R. Hogervorst and R. B. Helmholdt, Acta Crystallogr. Sect. B **44**, 120 (1988).

[6]S. Sawada, Y. Shiroishi, A. Yamamoto, M. Takashige, and M. Matsuo, J. Phys. Soc. Jpn. Lett. **43**, 2101 (1977); C. J. de Pater, Phys. Status Solidi A **48**, 503 (1978); R.P.A.R. van Kleef, Th. Rasing, J. H. M. Stoelinga, and P. Wyder, Solid State Commun. **39**, 433 (1981); T. Yamaguchi, S. Sawada, M. Takashige, and T. Nakamura, Jpn. J. Appl. Phys. **21**, L57 (1982).

[7]I. A. Belobrova, I. P. Aleksandrova, and A. K. Moskalev, Phys. Status Solidi A **66**, K17 (1981).

[8]Tokashi Ueda, Satoshi Iida, and Hikaru Terauchi, J. Phys. Soc. Jpn. **51**, 3953 (1982).

[9]M. Iizumi and K. Gesi, J. Phys. Soc. Jpn. **52**, 2526 (1983).

[10]J. F. Nye, *Physical Properties of Crystals* (Oxford University Press, Oxford, 1985), Chap. XIV.

[11]A. Janner and B. W. van Beest, in Proceedings of the XIth International Colloquium on Group Theoretical Methods in Physics, Istanbul, 1982 (unpublished).

[12]B. W. van Beest and A. Janner, Physica **122A**, 263 (1983).

[13]B. W. van Beest, A. Janner and R. Blinc, J. Phys. C **16**, 5409 (1983).

[14]Y. Uesu and J. Kobayashi, Ferroelectrics **64**, 115 (1985).

[15]R. A. Sanctuary, Ph.D. thesis, Eidgenössische Technische Hochschule–Zürich, 1985; results concerning the birefringence can also be found in P. Günter, R. Sanctuary, F. Rohner, H. Arend, and W. Seidenbusch, Solid State Commun. **37**, 883 (1981).

[16]See, for example, A. Sommerfeld, *Vorlesungen über Physik IV, Optik* (Geest & Portig, Leipzig, 1959), Chap. 4.

[17]V. A. Golovko and A. P. Levanyuk, Zh. Eksp. Teor. Fiz. **77**, 1556 (1979) [Sov. Phys.—JETP **50**, 780 (1979)].

[18]J. Fousek and J. Kroupa, Czech, J. Phys. B **36**, 1192 (1986).

[19]P. M. de Wolff, *Easy and Uneasy Superspace Groups,* lecture delivered at International Conference on Advanced Methods in X-ray and Neutron Analysis of Materials, Karlovy Vary, 1987 (unpublished).

[20]M. von Laue, *Röntgenstrahl Interferenzen* (Akademie-Verlag, Frankfurt, 1960).

[21]B. W. H. van Beest, Phys. Rev. B **33**, 960 (1986).

[22]Born, *Optik* (Springer-Verlag, Berlin, 1985).

[23]H. Meekes, Ph.D. thesis, University of Nijmegen, 1988.

[24]J. J. L. Horikx, Ph.D. thesis, University of Utrecht, 1987.

[25]W. J. Kusto, R. Struikmans, and B. Willemsen, in Proceedings of the Sixth European Meeting on Ferroelectrics, Poznań, 1987 [Ferroelectrics **80**, 289 (1988)].

[26]M. Régis, J. L. Ribet, and J. P. Jamet, J. Phys. (Paris) Lett. **43**, L333 (1982).

[27]M. Quilichini and J. Pannetier, Acta Crystallogr. Sect. B **39**, 657 (1983).

[28]K. Saito, T. Kawabe, and J. Kobayashi, Ferroelectrics **75**, 153 (1987).

[29]H. Mashyama, S. Tanisaki, and K. Hamano, J. Phys. Soc. Jpn. **50**, 2139 (1981).

[30]See, e.g., H. Kelker and R. Hatz, *Handbook of Liquid Crystals* (Verlag-Chemie, Weinheim-Deerfield, 1980), Chap. 7.